

c.1



LOAN COPY: RETURN
AFSWC (SWOIL)
KIRTLAND AFB, NM



TECH LIBRARY KAFB, NM

TECHNICAL NOTE

D-1317

DESIGN AND PERFORMANCE OF A LIQUID-HYDROGEN,
LIQUID-OXYGEN GAS GENERATOR FOR DRIVING
A 1000-HORSEPOWER TURBINE

By Nick J. Sekas and Loren W. Acker

Lewis Research Center
Cleveland, Ohio

NATIONAL AERONAUTICS AND SPACE ADMINISTRATION
WASHINGTON

July 1962



0153671

NATIONAL AERONAUTICS AND SPACE ADMINISTRATION

TECHNICAL NOTE D-1317

DESIGN AND PERFORMANCE OF A LIQUID-HYDROGEN,
LIQUID-OXYGEN GAS GENERATOR FOR DRIVING
A 1000-HORSEPOWER TURBINE

By Nick J. Sekas and Loren W. Acker

SUMMARY

The design and performance of a liquid-hydrogen, liquid-oxygen gas generator using several injector configurations and chamber lengths are presented. The results indicate that high combustion efficiency and reasonable gas temperatures can be achieved if a large number of annular injectors and chamber lengths of about 10 inches are used. Radial variations of gas temperature were observed in the combustion chamber and exhaust nozzle.

INTRODUCTION

The Lewis Research Center has been investigating the problems associated with the design and performance of a liquid-hydrogen, liquid-oxygen gas generator. This study was part of a rocket-system research program in which the function of the gas generator was to provide hot gas to drive a turbopump unit by utilizing the same propellants used to provide thrust. The system under consideration required a 1000-horsepower turbine to drive the pumps for pumping the propellants from the main tanks to the thrust chamber.

The feasibility of burning liquid hydrogen and liquid oxygen in gas generators to furnish hot gas in the range of 740° to 2160° R was reported in reference 1. In reference 1, difficulty was encountered in measuring the hot-gas temperatures. The temperature probes in the combustion chamber usually burned off flush with the wall and those downstream of the nozzle bent, lost their radiation shields, or failed in numerous other ways. Loss of the temperature probes was believed to have been caused by pure oxygen or streaks of hot gas resulting from inefficient propellant injection. Pure oxygen or streaks of hot gas at the exit of the gas generator could produce disastrous turbine-blade failures.

The objective of the current program was to develop a gas generator that would be reliable and controllable over a range of turbine-inlet conditions with emphasis on eliminating streaks of hot gas. The gas generator was intended to be of a preliminary design, from which a prototype flight configuration could be developed.

The gas generator was designed to operate at a total propellant flow rate of 0.890 pound per second and a combustion temperature and pressure of 1823° R and 240 pounds per square inch absolute, respectively. The oxidant- to fuel-weight ratio was to vary from approximately 0.5 to 1.2 over a total propellant flow rate of 0.42 to 0.92 pound per second.

The performance of the gas generator is presented for three injector configurations and several combustion-chamber lengths from 4 to 13 inches at Mach 0.15 chamber gas velocity. The elimination of the streaks of hot gas was investigated through variations in propellant injector design. Hot-gas temperatures obtained for one of the injector configurations are also presented.

SYMBOLS

| | |
|-------|---|
| A | cross-sectional area, sq in. |
| C_d | discharge coefficient |
| c^* | characteristic exhaust velocity, ft/sec |
| c_p | specific heat at constant pressure |
| d | diameter, in. |
| g | gravitational conversion factor, 32.2 ft/sec ² |
| h | enthalpy, Btu/lb |
| hp | horsepower |
| M | Mach number |
| M | molecular weight, lb/lb-mole |
| P | total pressure, lb/sq in. abs |
| R | universal gas constant, 1544 ft-lb/(lb)(°R) |
| T | total temperature, °R |

w weight flow, lb/sec
 γ ratio of specific heats
 η combustion efficiency, $c_{\text{actual}}^*/c_{\text{ideal}}^*$

Subscripts:

c chamber
 e exhaust
 f fuel
 o oxidant
 t total
 th throat

GAS-GENERATOR DESIGN CONSIDERATIONS

Ideal combustion properties for equilibrium composition during isentropic expansion were used for the design of the combustion-chamber and the combustion-chamber-nozzle flow areas. These properties are given in reference 2 and were extended to include the lower oxidant- to fuel-weight ratios required in this investigation. These properties are given graphically in figure 1.

The characteristic exhaust velocity c^* , which is frequently used in rocket analysis, is a property of the completely burned propellants. This parameter, defined as

$$c^* = \left[\frac{gRT}{\gamma \left(\frac{2}{\gamma + 1} \right)^{\frac{\gamma+1}{1-\gamma}}} \right]^{1/2} \quad (1)$$

is convenient for calculating the nozzle-throat area, as shown in the following equation:

$$A_{\text{th}} = \frac{c^* w_t}{P_t g} \quad (2)$$

The nozzle-throat area A_{th} in equation (1) must be corrected for flow coefficient in order to calculate the effective nozzle flow area. After this area is calculated, a chamber-exit Mach number is selected and the combustion-chamber flow area is calculated from the following equation:

$$A_c = \frac{C_d A_{th}}{M_c} \left[\frac{2 \left(1 + \frac{\gamma - 1}{2} M_c^2 \right)^{\frac{\gamma + 1}{2(\gamma - 1)}}}{\gamma + 1} \right] \quad (3)$$

The design calculations of the combustion chamber described herein are presented in the appendix.

The optimum combustion-chamber length is related to the propellant injector design and the chamber-exit gas velocity as discussed in reference 3. The injector design determines the degree of propellant atomization and mixing. A high degree of propellant atomization and the complete mixing of the propellants as close to the injector face as possible are necessary to eliminate the streaks of hot gas and to minimize the chamber length. A high chamber gas velocity is also desirable because it will increase the vaporization rate.

When the injection of the individual propellants is considered, oxygen, the more slowly vaporizing propellant, is the more critical. Maximum atomization and mixing of this propellant is necessary to obtain a homogeneous hot-gas mixture with the highest combustion efficiency. The atomization of the hydrogen is less critical. The results of reference 1 show that a failure occurred at the hydrogen injector face and resulted in a burn through to the fuel plenum that was not detected in the overall performance of the gas generator. This failure indicated that low hydrogen injector pressure drops are possible without affecting stability or combustion efficiency. The internal surface areas of both injector plenums should be minimized to prevent high heat transfer, which increases the required pressure drop to pass the required flow, especially during startup. During startup, the plenums are relatively hot compared with their normal operating temperatures, that is, 520° compared with 40° R for liquid hydrogen. Plenum pressures of sufficient magnitude could cause structural failures or adversely affect the propellant flow control system.

The ignition system is described in detail in reference 1. Ignition occurs during fuel lead, when the spark plug is energized and the main flow of liquid hydrogen and a small quantity of oxygen through the ground electrode are simultaneously introduced into the combustion chamber. A pilot flame is formed at the ground electrode, from which main combustion begins with the injection of liquid oxygen.

APPARATUS

The gas-generator research facility, the operating procedure, the propellant flow control, and the instrumentation used in this current investigation are the same as those described in detail in reference 1.

Gas Generator

A cross section of a typical gas-generator configuration used in this investigation (fig. 2) consisted of three components welded together to form the complete assembly. These components were the combustion chamber, the exhaust nozzle, and the propellant injector. A photograph of a typical assembly is shown in figure 3.

Combustion chamber. - The combustion chamber was made from a section of 2-inch, schedule 80, type 304 stainless-steel, seamless pipe. The inside diameter was machined to the design chamber diameter of 2.00 inches. Four combustion chambers were constructed with lengths of 4, 6, 11, and 13 inches.

Exhaust nozzle. - The Inconel exhaust nozzle had a throat diameter of 1.01 inches, which resulted in a nominal chamber-exit-gas Mach number of 0.15 for the 2.00-inch-diameter chamber. The approach contour to the nozzle throat was generated by the revolution of a quarter segment of an ellipse about the nozzle longitudinal axis. The exhaust nozzle length was 0.75 inch.

Propellant injector. - Three different injector configurations were used. The design of each succeeding injector configuration was based on the test results of the preceding configuration. All parts in the injector assembly were made from type 304 stainless steel. The oxygen orifices were copper brazed to the rear injector plate.

The first injector configuration tested, injector A, was used previously at the Lewis Research Center for the development of a gaseous-hydrogen, liquid-oxygen gas generator for driving research turbines (ref. 4). This injector face is shown in figure 4. The oxygen orifices of this injector were also brazed to the front injector plate. The oxygen was introduced through 12 orifices 0.035 inch in diameter. These orifices, located on a triangular pitch centered on the injector face, directed the oxygen flow parallel to the gas-generator axis. Immediately upstream of these orifices twisted metal strips (see fig. 2) were used to assist in the atomization of the liquid by inducing a tangential velocity component as it entered the combustion chamber. The hydrogen orifices of this injector were resized for use with the liquid instead of the gas. The hydrogen was introduced in three separate, but simultaneous, steps. The first step admitted 43 percent of the hydrogen

through three equally spaced 0.024-inch-diameter orifices surrounding each oxygen orifice and impinging on the oxygen jet at 30° . The impingement distance was $1/8$ inch from the injector face. The second step admitted 35 percent of the hydrogen through forty-two 0.20-inch-diameter orifices parallel to the combustion-chamber axis and surrounding the oxygen jets as shown in figure 4. The third step introduced the remaining 22 percent of the hydrogen parallel to the combustion-chamber axis through twenty-four 0.021-inch-diameter orifices located on the periphery of the injector face. The primary reason for the third step was to keep the chamber wall relatively cool by providing a hydrogen film between it and the hot core.

The second injector configuration, injector B (fig. 5), provided the same pattern and method of oxygen injection as injector A; however, the hydrogen injection pattern was changed to permit 90 percent of the liquid to flow through annular orifices that encircled each of the 12 oxygen jets. The remaining 10 percent of liquid was admitted around the periphery of the injector face as in injector A.

The third injector, injector C (fig. 6), is of the annular-flow type similar to injector B except that the number of oxygen orifices was doubled, while the pressure drop was maintained the same as in injector B. The pattern of the oxygen orifices was changed and wall cooling was eliminated. Twenty-four orifices were equally divided and spaced on three diameters. The diameters were so chosen that the oxygen orifices were located on centroids of equal areas in order to create a uniform oxidant flow over the cross section of the combustion chamber.

Ignition System

The ignition system was similar to that used in reference 1. The spark assembly was located within 1 inch of the injector face. A sectional view of the gas generator showing the orientation of the spark plug and the ground electrode (gaseous oxygen tube) is shown in figure 4. The spark gap was approximately $1/8$ inch.

Instrumentation

The instrumentation used in this investigation was the same as that in reference 1. Pressures were measured with linear variable-reluctance transducers. Liquid-hydrogen and liquid-oxygen temperatures were measured with carbon and platinum resistors, respectively. The hot-gas temperatures were measured with Chromel-Alumel thermocouples. The pressure-tap and thermocouple locations for a typical gas-generator configuration are shown in figure 2. The chamber-exit static pressure was measured approximately $1/8$ inch upstream of the approach contour of the

exhaust nozzle in all cases. Single thermocouples were placed in the center of the combustion chambers approximately 1 inch upstream of the nozzle throat for all gas generators using injector configurations A and B. With gas generators using injector configuration C, single thermocouples were placed 6 inches from the injector face at a radius of 1/4 inch from the chamber centerline, 9 inches from the injector face on the chamber centerline, 1/8 inch downstream on the centerline of the nozzle throat, and at the center of the 4-inch exhaust pipe 22 inches downstream of the injector face. For one run at a constant oxidant flow rate of 0.151 pound per second, the thermocouples were relocated to obtain radial temperatures in the combustion chamber and at the nozzle throat. All thermocouple locations are summarized in figure 7.

TEST CONDITIONS

Gas generators using propellant injectors A and B were tested at an oxidant- to fuel-weight ratio of approximately 1.0. The total propellant flow rate was varied between 0.42 and 0.92 pound per second. Chamber lengths of 4, 6, and 13 inches were used with injector configuration A. With injector B only 4- and 13-inch chamber lengths were used. The gas generator using injector C was tested at a constant oxidant flow rate of 0.151, 0.155, 0.228, and 0.231 pound per second and oxidant- to fuel-weight ratios between 0.490 and 1.88. The total propellant flow rate varied between 0.29 and 0.43 pound per second. The purpose of the tests with a fixed oxidant flow rate of 0.151 pound per second was to obtain the cross-sectional temperature distribution near the chamber exit and at the exhaust-nozzle throat. The chamber length for this gas generator was 11.0 inches. The duration of all runs of fixed propellant flow rate was 10 seconds.

RESULTS AND DISCUSSION

The gas generators operated smoothly during ignition and steady-state combustion. During startup, the steady-state pressures were reached within 1 second after ignition. Maximum pressure fluctuations were no greater than 1.5 percent of the average steady-state values. The injector plenum temperatures indicated liquid states for both propellants throughout every run.

Combustion Efficiency

The combustion efficiency, defined as the ratio of actual c^* to ideal c^* , was calculated in the same manner as described in reference 1. The actual c^* was computed from equation (2), in which the ideal ratio of specific heats is used to convert measured static pressure to total

pressure. The ideal c^* was obtained from figure 1 for the same oxidant- to fuel-weight ratio used in computing the actual c^* .

The principal data and calculated results obtained in the test program for injectors A and B are listed in table I. In figure 8, combustion efficiency is plotted as a function of the total propellant flow rate for three chamber lengths. The efficiency of the 13-inch-chamber-length gas generator averaged 0.992 for both injectors and was essentially independent of the total flow rate over the range of conditions tested. The shorter gas generators of 4- and 6-inch lengths resulted in efficiencies of approximately 0.95 for total flows between 0.60 and 0.92 pound per second. For lower flow rates, the efficiency decreased, and injector A produced a larger rate of decrease. These results indicated that for the 4- and the 6-inch lengths, annular injection was preferable to impingement injection for low flow rates. No measurement of combustion efficiency was made for injector C since high efficiency could be predicted for the long length and improved injector design used.

Hot-Gas Temperature

Although thermocouples were installed to measure hot-gas temperature at the chamber exit and at the exhaust-nozzle throat of the gas generators using injector configurations A and B, repeated thermocouple failures prevented temperatures from being measured. The thermocouples usually burned off flush with the chamber wall immediately after ignition. These failures were believed to have been caused by the inefficient atomization and vaporization of the liquid oxygen, which resulted in the consumption of the thermocouples by pure oxygen; thus, although combustion efficiencies were high for injectors A and B, they were not considered satisfactory for turbine application.

More uniform gas-temperature operation was obtained with the gas generator using injector C, as indicated by the fact that the thermocouples did not fail. This improved operation also indicated that doubling the number of oxygen orifices effectively improved atomization. The time-averaged values of hot-gas temperature obtained from the single thermocouple locations are listed in table II for the conditions tested.

The axial temperature variations of the hot gas for oxidant- to fuel-weight ratios of approximately 1.0 and 0.5 are plotted in figure 9 for three oxidant flow rates. The decrease in temperature in the direction of flow indicates the degree to which mixing of burned and unburned hydrogen was complete; that is, mixing was more complete at 9 inches from the injector face than at 6 inches. In addition to the effects of more complete mixing, some decrease in temperature with increase in axial distance was to be expected because of heat losses through the gas generator and exhaust-pipe wall, since neither the gas generator

nor the exhaust pipe were insulated. None of the ideal temperatures presented in this report has been corrected for this heat loss. The optimum chamber length based on these axial temperature measurements is the one at which the axial temperature profile crosses the ideal temperature. This is between 8 and 10 inches for the injector-C configuration.

At the highest flow rate, a slight temperature increase was observed between the combustion chamber and the exhaust pipe. Since the exhaust-pipe temperatures were approximately the same for all oxidant flow rates at the same oxidant- to fuel-weight ratios (table II), homogeneous mixing and complete combustion were believed to exist at this point. The lower temperature values in the combustion chamber and nozzle were therefore believed to be the result of a nonuniform cross-sectional temperature profile at these points that resulted from incomplete mixing of the propellants and/or incomplete combustion.

Gas-temperature uniformity was investigated by measuring temperatures at several radial positions 9 inches from the injector face in the combustion chamber and at the nozzle throat. The thermocouple locations for these measurements are shown in figure 7. Runs were made for a constant oxidant flow rate of 0.151 pound per second and oxidant- to fuel-weight ratios between 0.49 and 1.11. The temperatures resulting from these runs are presented in table III and are plotted in figure 10 against their respective oxidant- to fuel-weight ratios. The hot-gas temperatures obtained at the same distance from the injector face during the previous runs of constant oxidant flow at a slightly higher flow rate of 0.155 pound per second are included for comparison. The non-uniform temperature profile is evident. Temperature differences between measuring points in the combustion chamber were as low as 60° R at an oxidant- to fuel-weight ratio of 0.6 and as high as 320° R at an oxidant- to fuel-weight ratio of 0.95, and differences at the nozzle were as high as 470° R (fig. 10(b)).

The nonuniform temperatures were undoubtedly caused by localized areas of high and low oxidant flow. Such nonuniform flow resulted from a misalignment of the liquid-oxygen injector orifices that probably occurred during the brazing and/or welding of the injector assembly. After the completion of the test program the combustion chamber was separated from the injector assembly at the injector face. Water-spray tests showed this misalignment.

A compact gas generator similar to the one reported herein and using the injector-C configuration can be designed to provide satisfactorily the hot gas required to drive a turbopump unit of the power level prescribed. An injector redesign that doubles or triples the present number of 24 oxygen orifices may be beneficial for obtaining more uniform temperature distributions and possibly a shorter combustion chamber.

Wall-cooling orifices (as used in injectors A and B) are unnecessary for reliable operation since they were eliminated from injector C without detrimental effects to the combustion chamber.

SUMMARY OF RESULTS

Gas generators, 2 inches in diameter, that would generate a hot gas from a total liquid-oxygen and liquid-hydrogen flow rate of 0.890 pound per second at a combustion-chamber pressure of 240 pounds per square inch absolute and hot-gas temperature of 1823° R were designed, fabricated, and tested at oxidant- to fuel-weight ratios between 0.490 and 1.188 and total flow rates from 0.29 to 0.92 pound per second.

1. Combustion efficiencies were obtained for gas generators using two different types of propellant injector (one with 12 impinging injector orifices and the other with 12 annular injector orifices) and with combustion chamber lengths of 4, 6, and 13 inches. The 13-inch combustion chambers had a relatively constant efficiency of 0.992 over the range of propellant flow rates tested, whereas the 4- and 6-inch chambers produced a maximum efficiency of approximately 0.95. The impinging injector had a lower efficiency for the shorter length at the lower flow rates. Repeated thermocouple failures obtained for these configurations indicated excessive local gas temperatures.

2. A third injector, using 24 annular orifices with an 11-inch-combustion-chamber length, was designed and tested at constant oxidant flow rates of approximately 0.150 and 0.230 pound per second and oxidant- to fuel-weight ratios between 0.490 and 1.188. Hot-gas temperature measurements were obtained at 6 and 9 inches from the injector face at the nozzle outlet, and at the center of the exhaust pipe. A decrease in temperature in the direction of flow indicated more complete mixing of the burned and the unburned hydrogen. The optimum chamber length for complete mixing, based on the results of these temperature measurements, was between 8 and 10 inches. Sizable radial variations in temperature were observed at the 9-inch and the nozzle-outlet stations because of the misalignment of the oxygen-injector orifices. This misalignment occurred during the brazing and/or welding of the injector assembly.

3. Gas generators using a large number of annular orifices should be capable of producing hot gases for turbine drive applications with high combustion efficiency, uniform temperatures, and reasonable chamber lengths.

Lewis Research Center

National Aeronautics and Space Administration
Cleveland, Ohio, May 3, 1962

APPENDIX - GAS-GENERATOR DESIGN CALCULATIONS

The requirements for the design of a liquid-hydrogen, liquid-oxygen gas generator for producing a hot gas to drive a turbine are as follows:

| | |
|---|------|
| Turbine-inlet pressure, lb/sq in. abs | 240 |
| Hot-gas temperature, °R | 1823 |
| Output horsepower | 1000 |
| Turbine back pressure, lb/sq in. abs | 15 |
| Turbine efficiency | 0.45 |

From the design gas temperature, 1823° R, and figure 1, the following ideal combustion products parameters are obtained:

| | |
|---|------|
| Oxidant- to fuel-weight ratio | 1 |
| Characteristic exhaust velocity, c*, ft/sec | 6987 |
| Ratio of specific heats, γ | 1.36 |

The gas-generator design dimensions can therefore be obtained from the following calculations:

Turbine pressure ratio:

$$\frac{P_c}{P_e} = \frac{240}{15} = 16$$

Isentropic temperature ratio:

$$\begin{aligned} \frac{T_c}{T_e} &= \left(\frac{P_c}{P_e} \right)^{\frac{\gamma-1}{\gamma}} \\ &= (16)^{\frac{1.36-1}{1.36}} = 2.09 \end{aligned}$$

Ideal turbine-exhaust-gas temperature:

$$\begin{aligned} T_e &= \frac{T_c}{2.09} \\ &= \frac{1823}{2.09} = 872^\circ \text{ R} \end{aligned}$$

Ideal enthalpy change:

$$\begin{aligned}\Delta h &= c_p(T_c - T_e) \\ &= 1.86(1823 - 872) = 1768 \text{ Btu/lb}\end{aligned}$$

Total design weight flow:

$$\begin{aligned}w_t &= \left(\frac{\text{hp}}{\text{Turbine efficiency}} \right) \left(\frac{1}{\Delta h} \right) (0.707) \\ &= \left(\frac{1000}{0.45} \right) \left(\frac{1}{1768} \right) (0.707) = 0.890 \text{ lb/sec}\end{aligned}$$

For a turbine with a sonic-flow inlet nozzle the c^* relation is used for calculating the turbine-nozzle-throat area (gas-generator exhaust nozzle):

$$\begin{aligned}c^* &= \frac{P_t A_{th} C_d g}{w_t} \\ A_{th} C_d &= \frac{c^* w_t}{P_t g} \\ &= \frac{(6987)(0.890)}{(240)(32.2)} = 0.805 \text{ sq in.}\end{aligned}$$

For a nozzle with a circular flow area and a flow coefficient of 0.98, the nozzle-throat diameter is

$$\begin{aligned}d_{th} &= \left[\left(\frac{4}{\pi} \right) \left(\frac{1}{0.98} \right) (0.805) \right]^{1/2} \\ &= 1.02 \text{ in.}\end{aligned}$$

Approximate calculations indicated that a Mach 0.15 combustion-chamber gas velocity would result in an approximate 2-inch-diameter chamber. This chamber Mach number was therefore chosen because it permitted ample room for flexibility in the injector design. The ratio of

the combustion-chamber area to the nozzle-throat area is defined by the following equation:

$$\begin{aligned} \frac{A_c}{A_{th}C_d} &= \frac{1}{M_c} \left[\frac{2 \left(1 + \frac{\gamma - 1}{2} M_c^2 \right)}{\gamma + 1} \right]^{\frac{\gamma + 1}{2(\gamma - 1)}} \\ &= \frac{1}{0.15} \left\{ \frac{2 \left[1 + \frac{0.36}{2} (0.15^2) \right]}{1.36 + 1} \right\}^{\frac{1.36 + 1}{2(1.36 - 1)}} = 3.93 \end{aligned}$$

Therefore, the chamber diameter is

$$\begin{aligned} d_c &= \left[d_{th}^2 C_d \left(\frac{A_c}{A_{th}C_d} \right) \right]^{1/2} \\ &= \left[(1.02^2)(0.98)(3.93) \right]^{1/2} = 2.01 \text{ in.} \end{aligned}$$

REFERENCES

1. Acker, Loren W., Fenn, David B., and Dietrich, Marshall W.: Performance of a Small Gas Generator Using Liquid Hydrogen and Liquid Oxygen. NASA TM X-417, 1961.
2. Gordon, Sanford, and McBride, Bonnie J.: Theoretical Performance of Liquid Hydrogen and Liquid Oxygen as a Rocket Propellant. NASA MEMO 5-21-59E, 1959.
3. Clark, Bruce J., Hersch, Martin, and Priem, Richard J.: Propellant Vaporization as a Criterion for Rocket-Engine Design; Experimental Performance, Vaporization, and Heat-Transfer Rates with Various Propellant Combinations. NASA MEMO 12-29-58E, 1959.
4. Ball, Calvin L.: The Performance Evaluation of a Gaseous Hydrogen - Liquid Oxygen Gas Generator Designed for Driving Hot-Gas Research Turbines. Paper 61-WA-295, ASME, 1962.

TABLE I. - PERFORMANCE OF IMPINGING INJECTOR A AND ANNULAR INJECTOR B

[Chamber diameter, 2.00 in.; nozzle diameter, 1.01 in.; nozzle discharge coefficient, 0.982; 12 oxygen orifices.]

| Run | Chamber length, in. | Total flow, lb/sec | Oxidant- to fuel-weight ratio | Fuel flow, lb/sec | Chamber-exit total pressure, lb/sq in. abs | Liquid-oxygen injector temperature, °R | Fuel injector temperature, °R | Liquid-oxygen injector total-pressure difference, lb/sq in. | Fuel injector total-pressure difference, lb/sq in. | Combustion efficiency |
|---------------------------------|---------------------|--------------------|-------------------------------|-------------------|--|--|-------------------------------|---|--|-----------------------|
| Injector A (impinging injector) | | | | | | | | | | |
| 1 | 4.0 | 0.806 | 1.05 | 0.394 | 210 | 188 | 50 | 113 | 12 | 0.945 |
| 2 | ↓ | .920 | 1.05 | .450 | 240 | 186 | 49 | 122 | 16 | .946 |
| 3 | ↓ | .616 | 1.07 | .298 | 161 | 181 | 50 | 70 | 8 | .948 |
| 4 | ↓ | .524 | 1.09 | .251 | 133 | 177 | 50 | 56 | 6 | .920 |
| 5 | ↓ | .422 | 1.13 | .198 | 104 | 176 | 51 | 42 | 4 | .870 |
| 6 | 6.0 | .811 | 1.04 | .397 | 214 | 187 | 49 | 107 | 10 | .958 |
| 7 | ↓ | .911 | 1.05 | .445 | 236 | 183 | 49 | 122 | 14 | .940 |
| 8 | ↓ | .618 | 1.04 | .303 | 161 | 182 | 49 | 65 | 4 | .945 |
| 9 | ↓ | .524 | 1.04 | .257 | 137 | 179 | 49 | 48 | 2 | .945 |
| 10 | ↓ | .432 | 1.04 | .212 | 109 | 179 | 50 | 41 | 5 | .911 |
| 11 | 13.0 | .804 | 1.01 | .400 | 219 | 176 | 50 | 108 | 15 | .986 |
| 12 | ↓ | .898 | 1.02 | .445 | 247 | 176 | 50 | 120 | 20 | .996 |
| 13 | ↓ | .607 | 1.00 | .304 | 167 | 174 | 51 | 66 | 15 | .996 |
| 14 | ↓ | .513 | 1.00 | .257 | 141 | 175 | 51 | 52 | 14 | .991 |
| 15 | ↓ | .424 | 1.03 | .209 | 116 | 175 | 51 | 45 | 10 | .991 |
| Injector B (annular injector) | | | | | | | | | | |
| 16 | 4.0 | 0.814 | 1.07 | 0.393 | 218 | --- | -- | --- | -- | 0.956 |
| 17 | ↓ | .911 | 1.07 | .441 | 244 | --- | -- | --- | -- | .959 |
| 18 | ↓ | .618 | 1.09 | .298 | 166 | --- | -- | --- | -- | .958 |
| 19 | ↓ | .529 | 1.12 | .250 | 141 | --- | -- | --- | -- | .945 |
| 20 | ↓ | .430 | 1.13 | .202 | 114 | --- | -- | --- | -- | .935 |
| 21 | 13.0 | .804 | 1.02 | .398 | 219 | 198 | 49 | 98 | 45 | .988 |
| 22 | ↓ | .904 | 1.04 | .444 | 246 | 192 | 48 | 109 | 50 | .985 |
| 23 | ↓ | .611 | 1.02 | .303 | 167 | 184 | 48 | 63 | 34 | .990 |
| 24 | ↓ | .519 | 1.03 | .256 | 139 | 182 | 49 | 50 | 31 | .970 |
| 25 | ↓ | .420 | 1.03 | .207 | 114 | 180 | 49 | 42 | 28 | .985 |

TABLE II. - COMBUSTION PRODUCTS TEMPERATURE MEASUREMENTS

[Injector C (annular injector); 24 oxygen orifices; chamber diameter, 2.00 in.; nozzle diameter, 1.01 in.; chamber length, 11 in.]

| Run | Oxidant flow rate, lb/sec | Oxidant- to fuel-weight ratio | Combustion temperature (thermo-couple 1 ^a), °R | Combustion temperature (thermo-couple 2 ^a), °R | Nozzle-throat temperature (thermo-couple 3 ^a), °R | Exhaust-pipe temperature (thermo-couple 4 ^a), °R | Theoretical combustion temperature, °R |
|-----|---------------------------|-------------------------------|--|--|---|--|--|
| 26 | 0.155 | 0.506 | 880 | 885 | 850 | 810 | 960 |
| 27 | ↓ | .613 | 1200 | 1090 | 1040 | 995 | 1155 |
| 28 | ↓ | .795 | 1660 | 1320 | 1340 | 1250 | 1475 |
| 29 | ↓ | 1.000 | 2330 | 1845 | 1740 | 1500 | 1823 |
| 30 | ↓ | 1.140 | 2575 | 2025 | 1950 | 1690 | 2050 |
| 31 | .228 | .492 | 1160 | 810 | 725 | 790 | 945 |
| 32 | ↓ | .594 | 1390 | 960 | 925 | 965 | 1120 |
| 33 | ↓ | .794 | 1940 | 1230 | 1290 | 1275 | 1475 |
| 34 | ↓ | .996 | 2455 | 1435 | 1590 | 1565 | 1810 |
| 35 | ↓ | 1.188 | 2945 | 1605 | 1840 | 1830 | 2120 |
| 36 | .231 | .498 | 925 | 710 | 695 | 785 | 945 |
| 37 | ↓ | .597 | 1230 | 880 | 855 | 960 | 1130 |
| 38 | ↓ | .802 | 1880 | 1150 | 1125 | 1260 | 1470 |
| 39 | ↓ | 1.004 | 2415 | 1490 | 1390 | 1575 | 1825 |
| 40 | ↓ | 1.185 | ---- | 1665 | 1640 | 1800 | 2130 |

^aSee fig. 7.

TABLE III. - RADIAL TEMPERATURE MEASUREMENTS 9 INCHES FROM

INJECTOR FACE AND AT NOZZLE THROAT FOR INJECTOR C

[Oxidant flow rate, 0.151 lb/sec.]

| Oxidant- to fuel-weight ratio | Combustion temperature, °R, at thermocouple ^a - | | | | | | Theoretical combustion temperature, °R |
|-------------------------------------|---|------|------|------|------|------|---|
| | 2 | 5 | 6 | 7 | 8 | 9 | |
| 0.490 | 870 | 740 | 920 | 870 | 640 | 700 | 940 |
| .594 | 1080 | 1025 | 1030 | 1050 | 970 | 880 | 1120 |
| .774 | 1420 | 1300 | 1375 | 1460 | 1155 | 1200 | 1430 |
| .950 | 1980 | 1665 | 1745 | 1980 | 1350 | 1690 | 1730 |
| 1.110 | 2100 | 1960 | 2085 | 1950 | 1540 | 2010 | 2010 |

^aSee fig. 7.

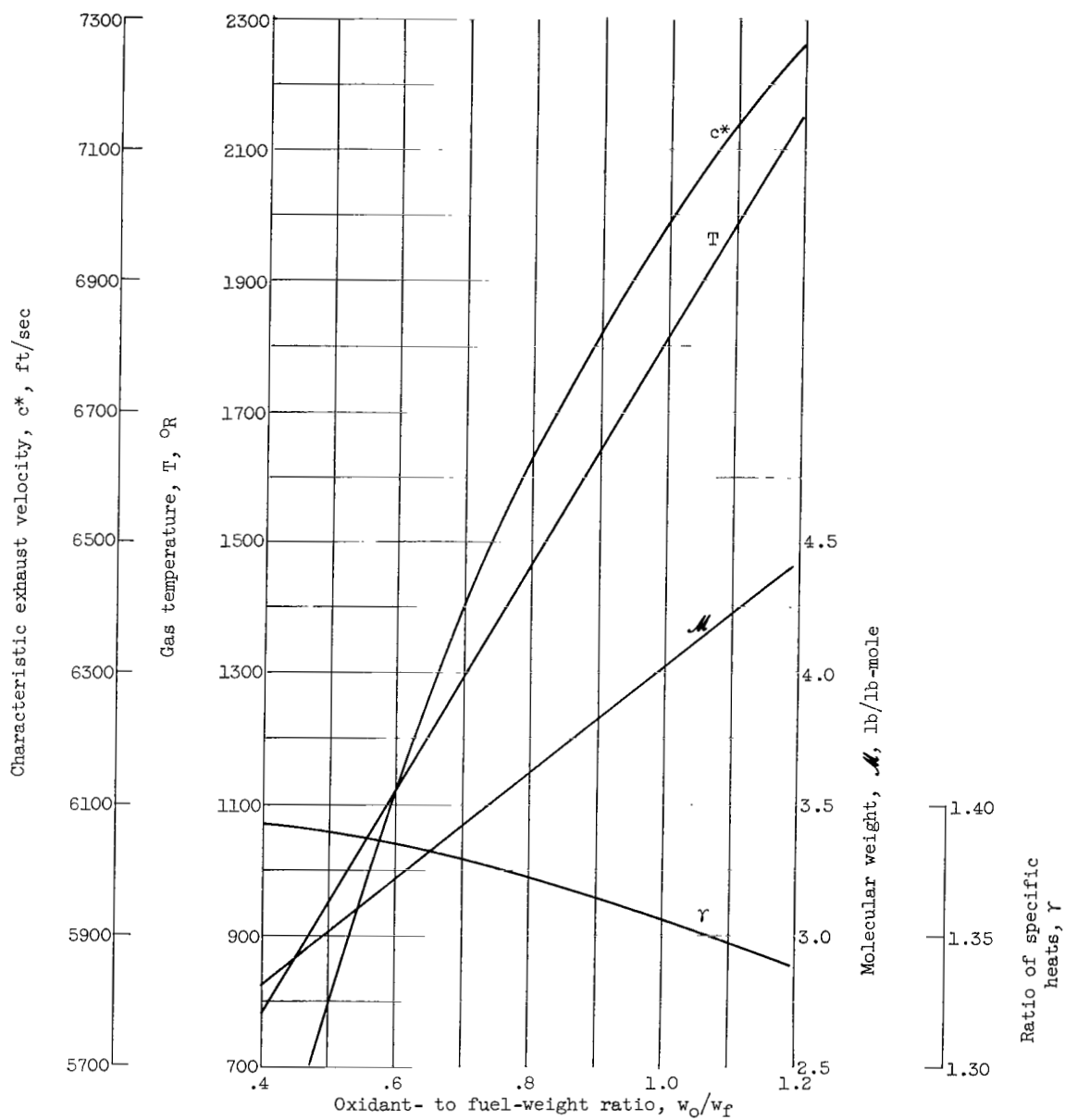
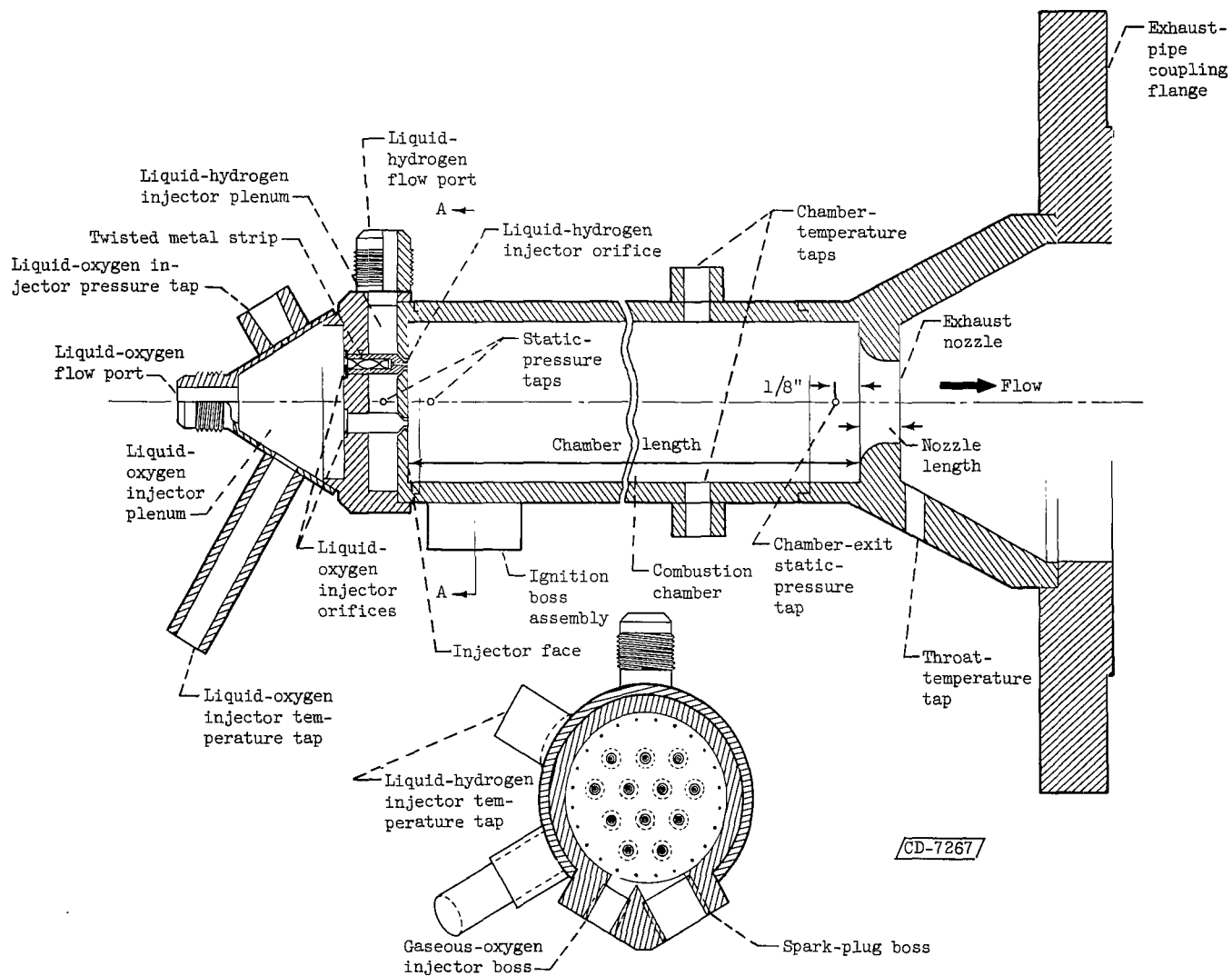
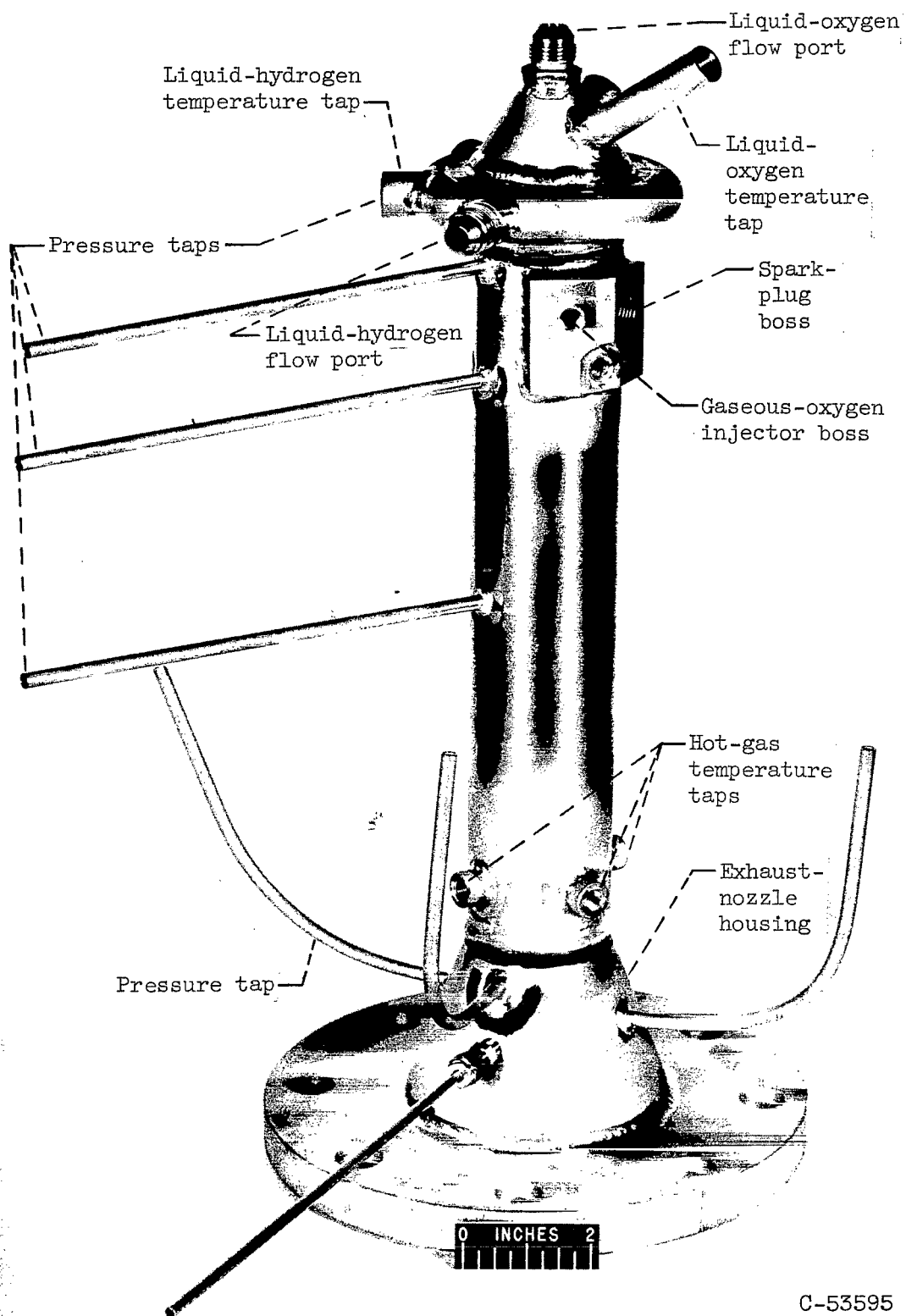


Figure 1. - Ideal combustion properties of liquid hydrogen and liquid oxygen (ref. 2).



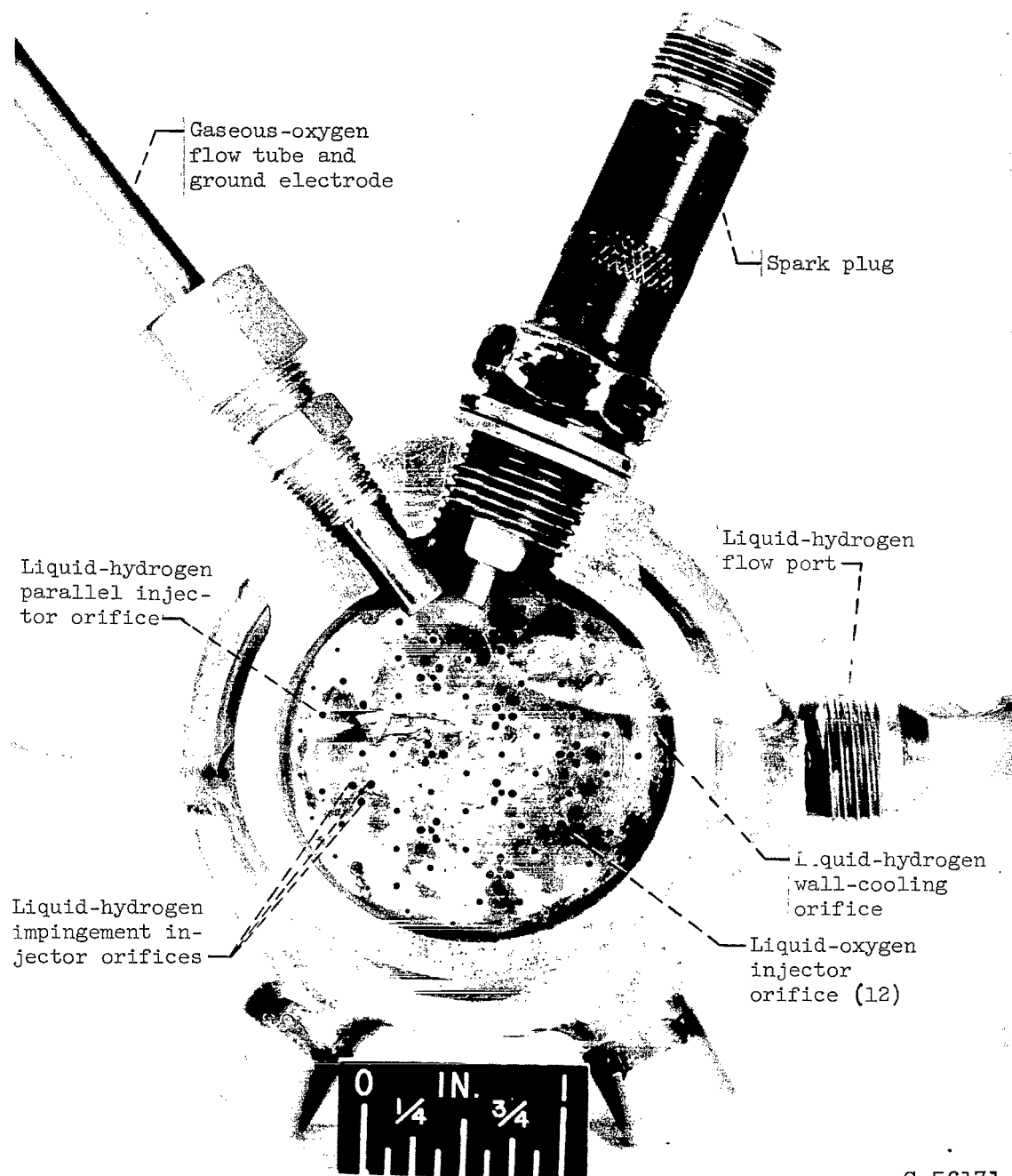
Section A-A

Figure 2. - Gas-generator cross section.



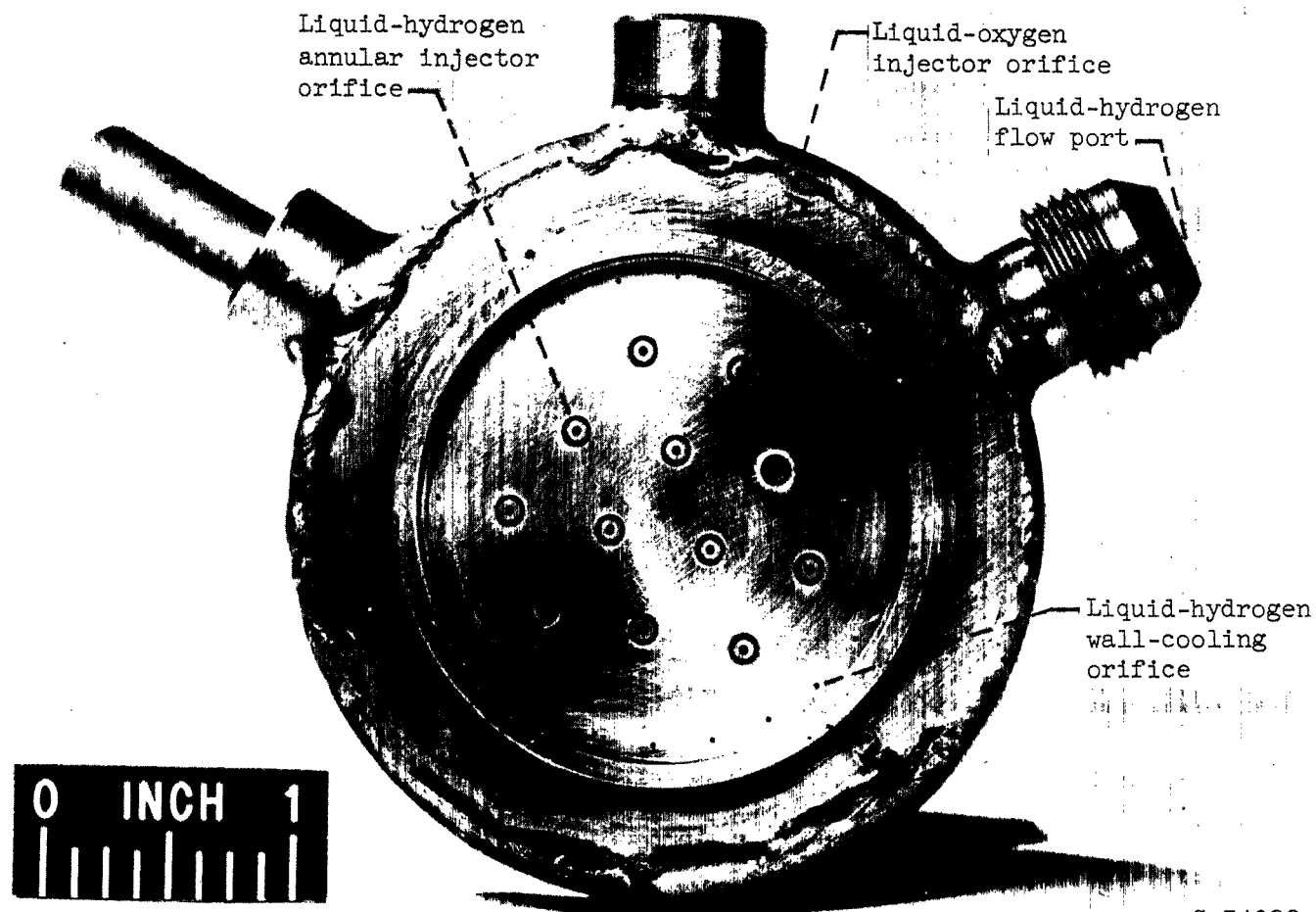
C-53595

Figure 3. - Gas-generator assembly.



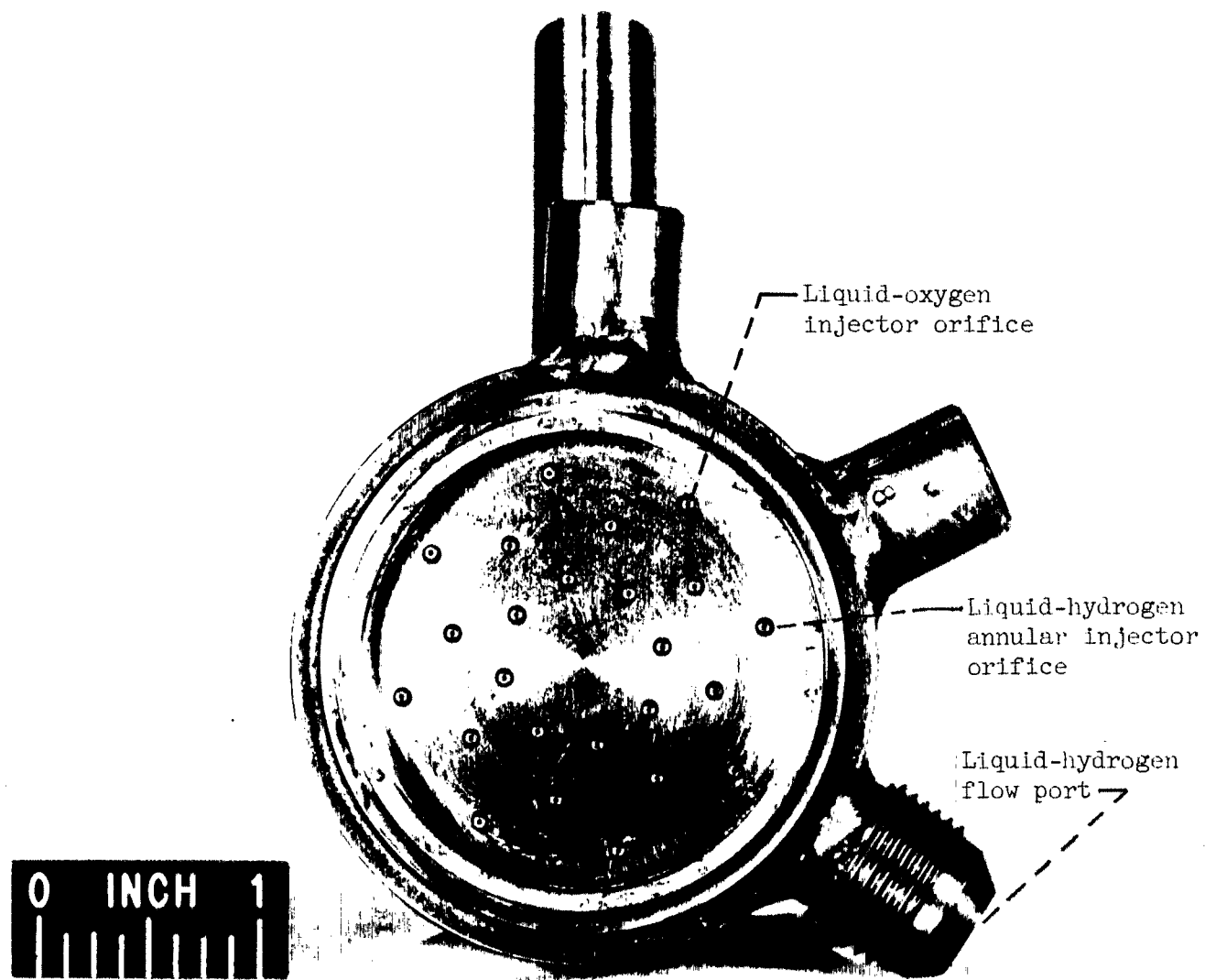
C-56171

Figure 4. - Propellant injector A; impinging injector with wall cooling.



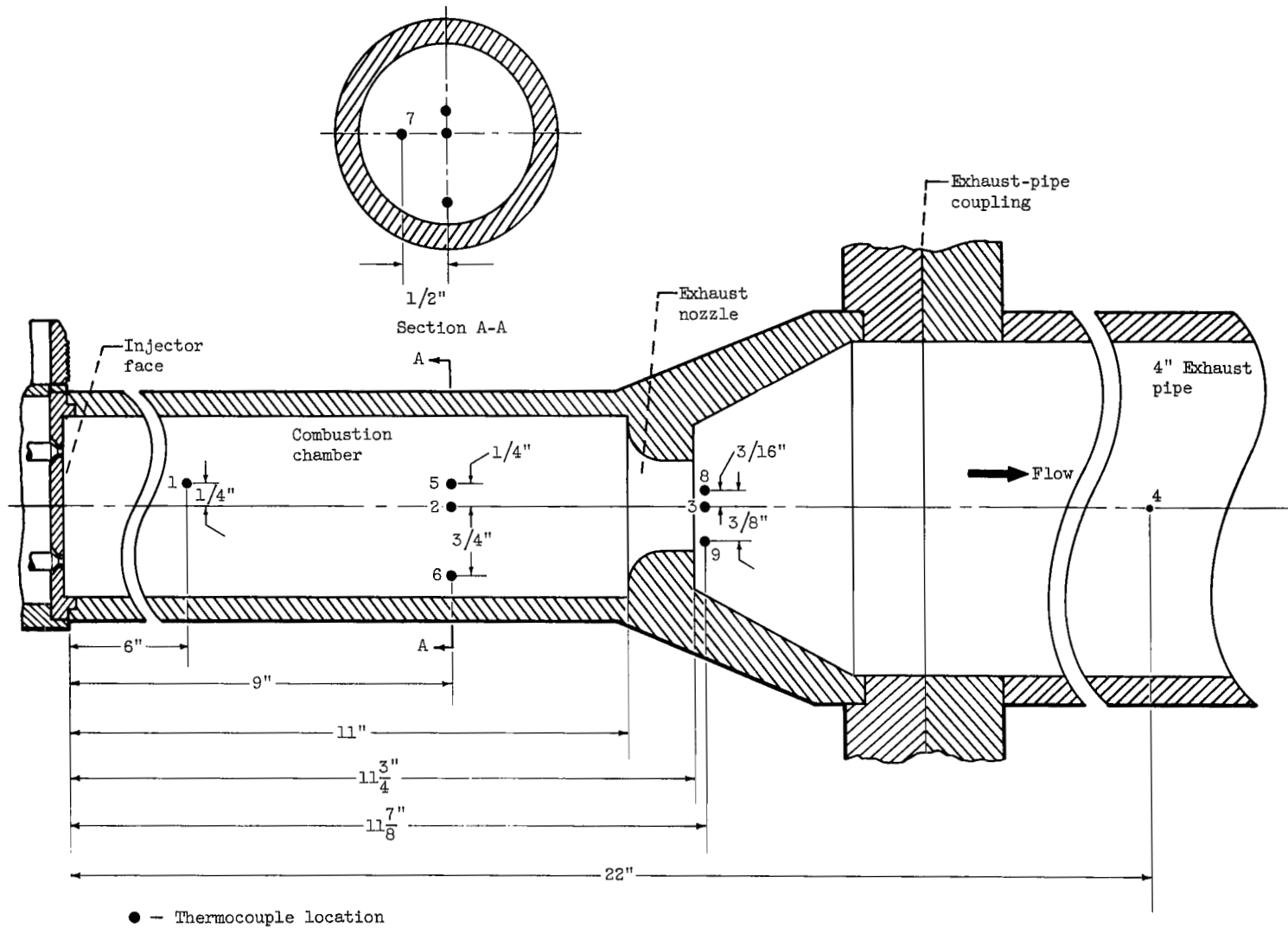
C-54026

Figure 5. - Propellant injector B; annular injector with wall cooling.



C-55183

Figure 6. - Propellant injector C; annular injector without wall cooling.



CD-7381

Figure 7. - Location of hot-gas temperature measurements for injector-C configuration.

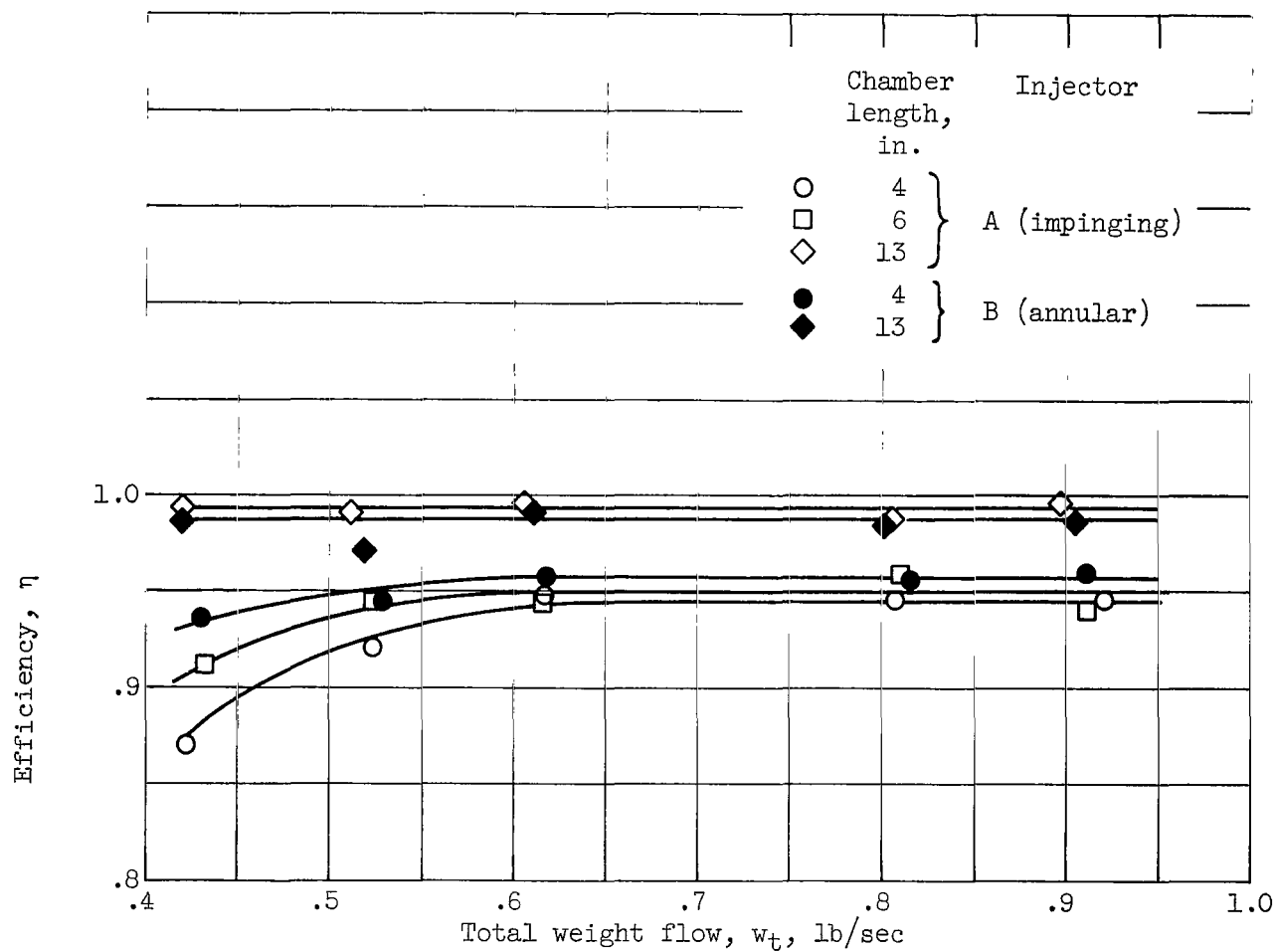
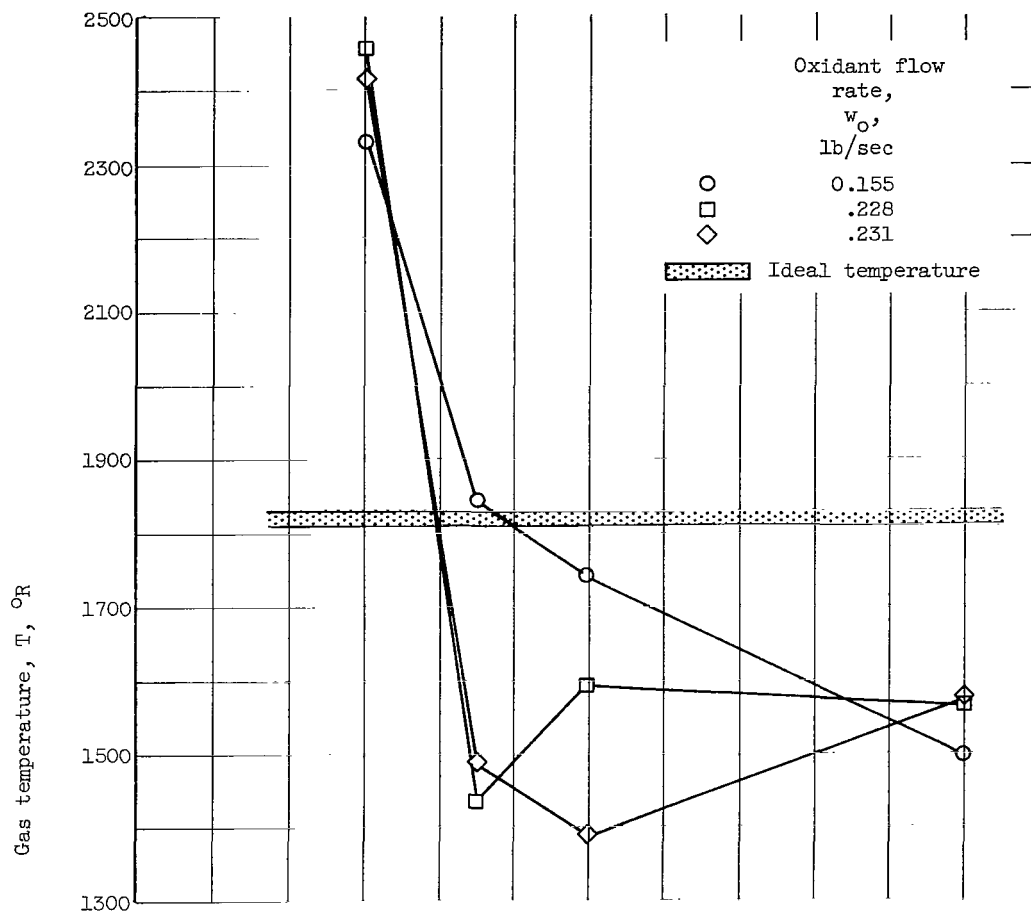
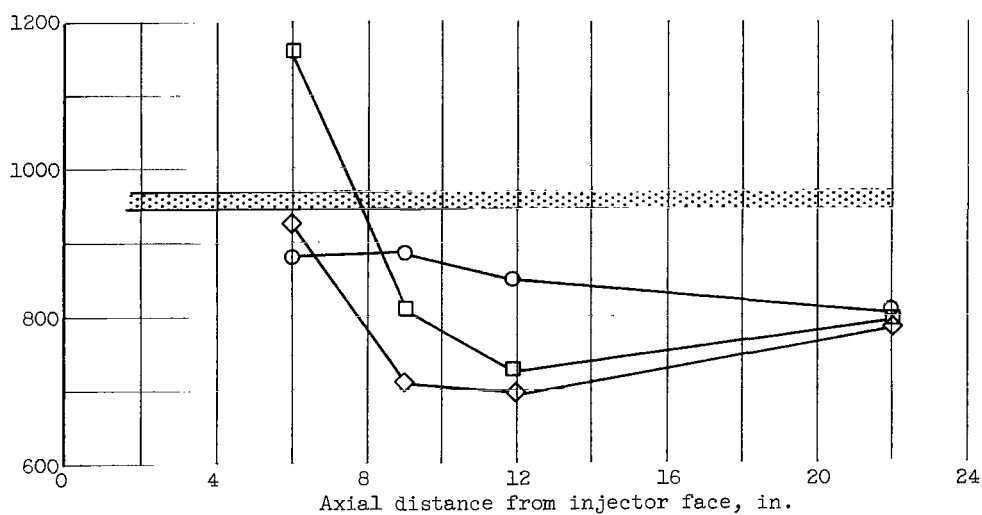


Figure 8. - Variation of combustion efficiency with total weight flow at oxidant- to fuel-weight ratios between 1.00 and 1.13.



(a) Oxidant- to fuel-weight ratio, approximately 1.0.



(b) Oxidant- to fuel-weight ratio, approximately 0.5.

Figure 9. - Axial temperature measurements at constant oxygen flow for injector C.

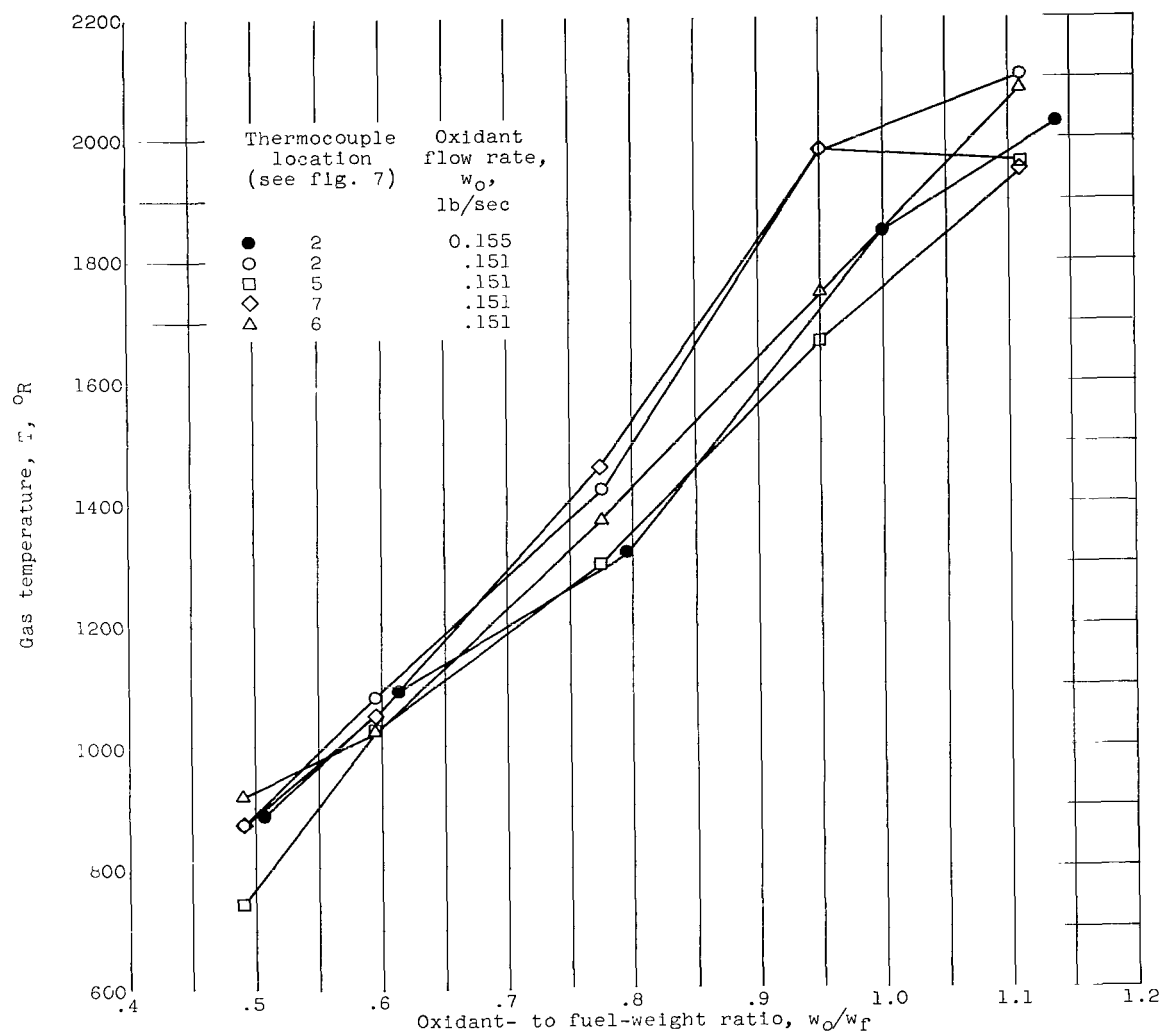
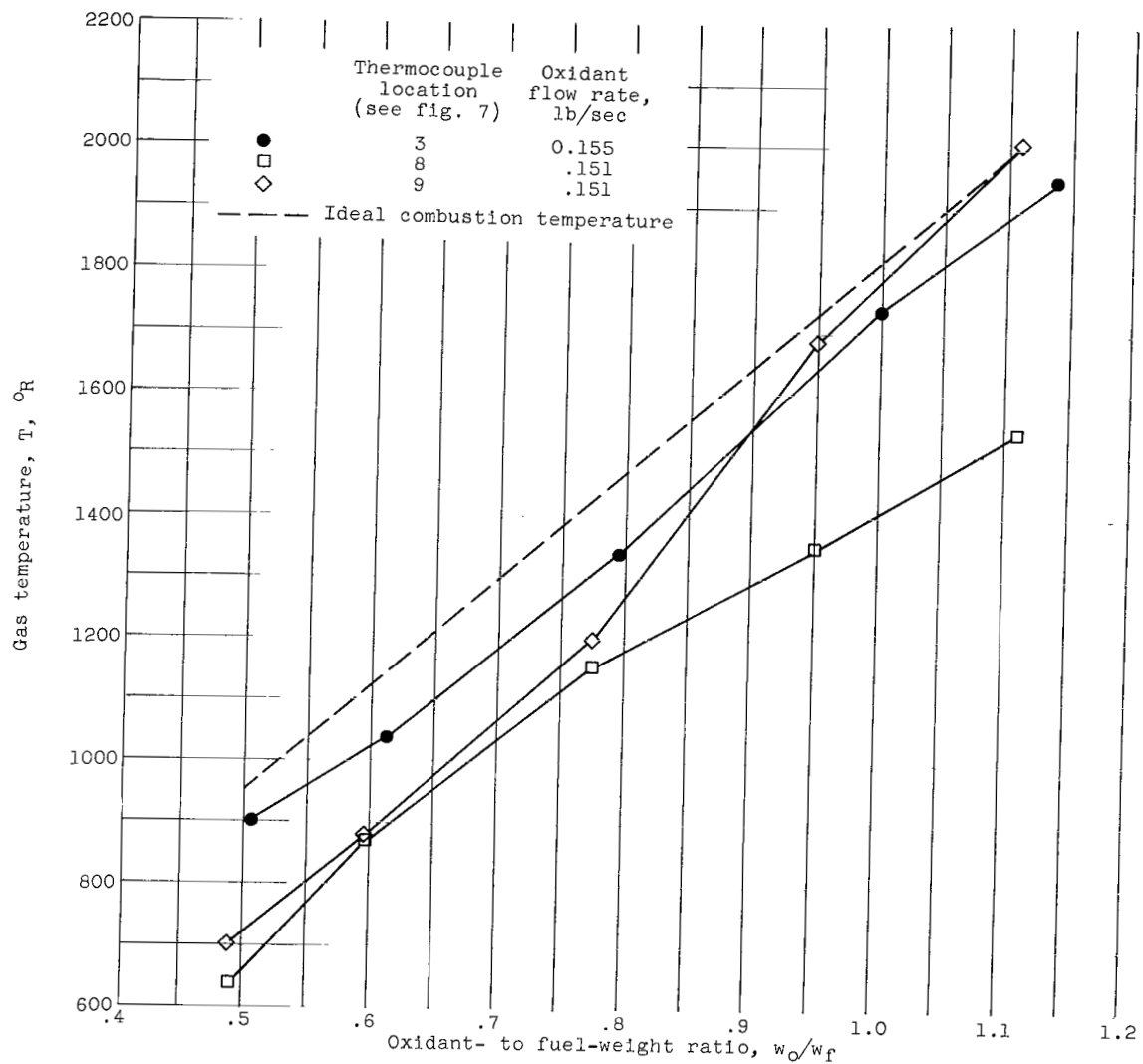


Figure 10. - Hot-gas temperatures for injector C.



(b) Measurements at nozzle throat.

Figure 10. - Concluded. Hot-gas temperatures for injector C.